Denoising 3D Medical Images Using a Second Order Variational Model and Wavelet Shrinkage

Minh-Phuong Tran[1], Renaud Péteri[2], and Maitine Bergounioux[1]

[1] Université d'Orléans, Laboratoire MAPMO
UMR 6628, Fédération Denis-Poisson
BP 6759, F-45067 Orléans Cedex 2, France
minh-phuong.tran@etu.univ-orleans.fr, Maitine.Bergounioux@univ-orleans.fr
[2] Université de La Rochelle,
Laboratoire Mathématiques, Image et Applications
EA 3165
F-17000 La Rochelle, France
renaud.peteri@univ-lr.fr

Abstract. The aim of this paper is to construct a model which decomposes a 3D image into two components: the first one containing the geometrical structure of the image, the second one containing the noise. The proposed method is based on a second order variational model and an undecimated wavelet thresholding operator. The numerical implementation is described, and some experiments for denoising a 3D MRI image are successfully performed. Future prospects are finally exposed.

Keywords: Image Decomposition, Image Denoising, Undecimated wavelet Shrinkage, Second order variational model, 3D medical image.

1 Introduction

Medical images obtained from MRI (Magnetic-Resonance-Imaging) are now a very common tool for diagnosing human diseases. These images are often affected by random noise arising during the acquisition process. Moreover, medical images constituted of low-contrast objects are a major challenge for biomedical researchers. The noise highly affects the visual interpretation of medical images, but also most of the segmentation or clustering algorithms. Therefore, denoising medical images is an important pre-step for medical image analysis.

Image denoising is one of the classical problems in image processing, and has been studied for several years due to its important role in various applications. Its goal is to remove noise and/or spurious details from a given corrupted image while maintaining its important features. Many denoising methods have been developed, such as methods based on variational methods, rank filters, frequency domain filters or sparse representations (curvelets, beamlets,...).

The general idea behind variational denoising methods is to considered an observed image f as a corrupted version of a noiseless image u. In denoising models, image u is then the solution of an inverse problem. One of the most successful variational algorithms is the Rudin-Osher-Fatemi (ROF) model ([2,4,5]) which uses Total-Variation regularization. The observed image to recover/denoise f is

split into two components u and v, giving $f = u + v$, where u is the cartoon part (the smooth component), the remaining term $v := f - u$ being the noise. The functional energy F on bounded variation space is:

$$F(u) = \frac{1}{2} \|f - u\|_{L^2(\Omega)}^2 + \lambda TV(u), u \in BV(\Omega) \tag{1}$$

where $TV(u)$ represents the total variation of $u \in BV(\Omega)$ [10], and $\lambda \geq 0$ is a regularization parameter. Solving this problem leads to the minimisation of the following expression:

$$\inf_{u \in BV(\Omega)} F(u) \tag{$\mathcal{P}_{ROF}$}$$

It has been shown that this problem has a unique solution in $BV(\Omega)$ ([9,1]). However, the use of the BV-norm in the ROF model favours piecewise constant solutions, causing unsatisfying *'staircasing effects'* [6]. This variational model has been improved by using different functional spaces. In [9] it has been proposed to use the second order functional space of bounded variation - the BV^2 space. This model leads to the minimisation of the following expression:

$$\inf_{u \in BV^2(\Omega)} F_2(u) \tag{$\mathcal{P}_{ROF2}$}$$

where

$$F_2(u) = \frac{1}{2} \|f - u\|_{L^2(\Omega)}^2 + \lambda TV^2(u), u \in BV^2(\Omega) \tag{2}$$

In the following section, we generalize the model ROF to the new functional space BV^2 for 3D signals using second order total variation TV^2 [10]. The problem is considered in the BV^2 discrete space.

2   Three-Dimensional ROF2 Model

2.1   Functional Framework

Let $\Omega \subset \mathbb{R}^3$ be an open bounded set, we consider the finite-dimensional problem where function F_{ROF2}:

$$\begin{aligned} F_{ROF2} : BV^2(\Omega) &\to \mathbb{R}^+ \\ u &\mapsto F_{ROF2}(u) \end{aligned}$$

is defined by:

$$F_{ROF2}(u) = \frac{1}{2} \|f - u\|_{L^2(\Omega)}^2 + \lambda TV^2(u)$$

Solving the second order model (ROF2) leads to the minimisation of the following expression:

$$\inf_{u \in BV^2(\Omega)} \frac{1}{2} \|f - u\|_{L^2(\Omega)}^2 + \lambda TV^2(u) \tag{$\mathcal{P}_{ROF2}$}$$

Theorem 1. [9] *If $\lambda > 0$, it has been shown that the problem has an unique solution.*

2.2   Discretization of the ROF2 Model

In the sequel, we denote by X the Euclidean space $\mathbb{R}^{N_1 \times N_2 \times N_3}$ and $Y = X \times X \times X$. The space X is endowed with the inner product:

$$\langle u, v \rangle_X = \sum_{\substack{1 \leq i \leq N_1 \\ 1 \leq j \leq N_2 \\ 1 \leq k \leq N_3}} u_{i,j,k} v_{i,j,k}$$

In the case of the ROF2 model, the second order total variation term $TV^2(u)$ can be discretized to $J(u)$ (more details can be found in [9,10]). The discretization of the ROF2 model ($\mathcal{P}_{ROF2}$) can be then defined as:

$$\inf_{u \in X} J(u) + \frac{1}{2\lambda} \|f - u\|_X^2 \qquad \text{(d-}\mathcal{P}_{ROF2})$$

where $J(u)$ stands for the discrete TV^2. The following theorem comes from the convex duality theory [7], and gives the approximated solution:

Theorem 2. *The solution to problem ROF2 verifies:*

$$u = f - P_{\lambda K}(f)$$

where $P_{\lambda K}$ is the orthogonal projector operator on λK, and

$$K := \{H^* p \mid p \in X^9, \ \|p_{i,j,k}\|_{\mathbb{R}^9} \leq 1; \ 1 \leq i, j, k \leq N_1, N_2, N_3\}.$$

H is the Hessian operator and H^* its adjoint. We refer to [9,2] for the proof of this theorem. Moreover, in order to approximate the projection term $P_{\lambda K}(f)$ of theorem 2, the following problem has to be solved [2] :

$$\begin{cases} \min \|\lambda H^* p - f\|_X^2 \\ p \in X^9 \\ \|p_{i,j,k}\|_{\mathbb{R}^9}^2 \leq 1; 1 \leq i, j, k \leq N_1, N_2, N_3 \end{cases} \qquad (3)$$

This problem can be solved by a fixed point method with an iterative scheme on the solution p: $p^0 = 0$ and

$$p_{i,j,k}^{n+1} = \frac{p_{i,j,k}^n - \tau \left(H \left[H^* p^n - \frac{f}{\lambda} \right] \right)_{i,j,k}}{1 + \tau \left\| \left(H \left[H^* p^n - \frac{f}{\lambda} \right] \right)_{i,j,k} \right\|_{\mathbb{R}^9}} \qquad (4)$$

The discretization of the three-dimensional Hessian operator H and its adjoint operator H^* as well as a sufficient condition ensuring the convergence of the algorithm can be found in [10].

Theorem 3. [10] *Let $\tau \leq 1/12^2$, then $\lambda(H^* p^n)_n$ converges to $P_{\lambda K}(f)$ as $n \to \infty$.*

3 3D Image Decomposition Model Using Undecimated Wavelet Shrinkage

In this section, a decomposition model based on the second order variational model ROF2 is presented. Following the work of [15,8], an undecimated wavelet transform (the 'a trous' algorithm) is introduced in order to better separate geometry from noise during the iteration process.

3D Decomposition Model. The proposed method aims at dividing a 3D image f into two components: the first component $u \in BV^2$ represents the geometrical information (smooth part) while the second component v contains the noise, with $f = u+v$. This decomposition model has been proposed in [8] and is computed by minimizing a convex functional which depends on two variables (u, v) as following:

$$\inf_{(u,v)\in X^2} J(u) + B^*(v/\delta) + \frac{1}{2\lambda} \|f - u - v\|_X^2 \qquad (\mathcal{P})$$

where $B^*(v/\delta)$ is the Legendre-Fenchel transform of B of the noise component v, [8]. Furthermore, let us denote $\delta B_E = \{z/\|z\|_E \leq \delta\}$. In order to solve the problem $(\mathcal{P})$, one considers to solve the two following problems:

1. v being fixed, we find u as solution of problem:

$$\inf_{u\in X} J(u) + \frac{1}{2\lambda} \|f - u - v\|_X^2 \qquad (5)$$

2. u being then fixed, we search for v as the solution of:

$$\inf_{v\in \delta B_E} \|f - u - v\|_X^2 \qquad (6)$$

The solution of problem (5) is given by $u^* = f - v - P_{\lambda K}(f - v)$.

Solution of (6) is obtained using the universal threshold T during the iteration process [8] on an undecimated wavelet transform, the 'à trous' algorithm. Solution can be written $v^* = f - u - UWT(f - u, T)$, where UWT denotes the undecimated wavelet thresholding operator that is detailed in the next section.

The " à trous" Algorithm. The 'à trous' algorithm [3] is a fast dyadic wavelet transform and is implemented with filter banks. It is similar to a fast biorthogonal wavelet transform but without subsampling. In our 3D implementation, the scaling and wavelet functions ϕ and ψ are a cubic B-splines that enable a nearly isotropic analysis of the 3D image, and filters are separable 1D filters.

For any resolution level $j \geq 0$, the approximation a_j and the details d_j (wavelet coefficients) are:

$$a_j[n, m, l] = \;< f(x, y, z), \phi_{2^j}(x - n)\phi_{2^j}(y - m)\phi_{2^j}(z - l) > \qquad (7)$$
$$d_j[n, m, l] = \;< f(x, y, z), \psi_{2^j}(x - n)\psi_{2^j}(y - m)\psi_{2^j}(z - l) > \qquad (8)$$

and discrete image values are assimilated to $a_0[n, m, l]$.

A filter $x[n]$ is dilated to make the filter $x_j[n]$ by inserting 2^{j-1} zeros ('trous') between each sample. Let us denote $\bar{x}_j[n] = x_j[-n]$ and $\delta[n]$ the discrete Dirac. $\bar{h}$ is a low-pass filter associated with the scaling function ϕ and $\bar{g}$ is a high-pass filter associated with the mother wavelet ψ.

The "à trous" algorithm then enables to compute the fast dyadic wavelet transform in the following way:

$$a_{j+1}[n, m, l] = (\bar{h}_j \bar{h}_j \bar{h}_j * a_j)[n, m, l], \qquad (9)$$
$$d_{j+1}[n, m, l] = ([\bar{h}_j \bar{h}_j \bar{h}_j - \delta\delta\delta] * a_j)[n, m, l] \qquad (10)$$

where $\bar{h}_j \bar{h}_j \bar{h}$ and $\delta\delta\delta$ are 3D filters obtained from $\bar{h}$ and δ by tensor products.

As there is no downsampling of the original image, all the approximation and wavelet images have the same size. The undecimated wavelet thresholding operator UWT used for computing v^* perform the 3D 'à trous' decomposition of the image, applies the universal threshold T on each 3D wavelet images and reconstructed the 3D thresholded image by summing the details and the last approximation.

Proposed Algorithm. Consequently, our decomposition model is solved by the following iterative algorithm:

1. Initialization: $u_0 = v_0 = 0$,
2. Iterations on n:
$$u_{n+1} = f - v_n - P_{\lambda K}(f - v_n) \qquad (11)$$

$$v_{n+1} = f - u_{n+1} - UWT(f - u_{n+1}, T) \qquad (12)$$

3. Stopping test: if the following condition is fullfilled:

$$\max\left(|u_{n+1} - u_n|, |v_{n+1} - v_n|\right) \le \epsilon \qquad (13)$$

4   Application to 3D Medical Image Denoising

The proposed method has been applied on the MRI of a trisomic mouse (Fig. 1). The mouse brain volume is the stack of 104 MRI images. This is a difficult case because the contrast between different objects in the brain is low, and there is moreover some acquisition noise (see top image of figure 3).

Our 3D image decomposition method has been applied to this data, for different values of regularizing parameter λ (see figure 2). Since in practice there is no denoised volume to compare to, tuning of parameter λ often relies on visual inspection. The stopping criterion has been set to a maximal number of iterations which can be chosen arbitrary large.
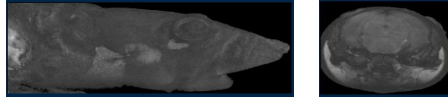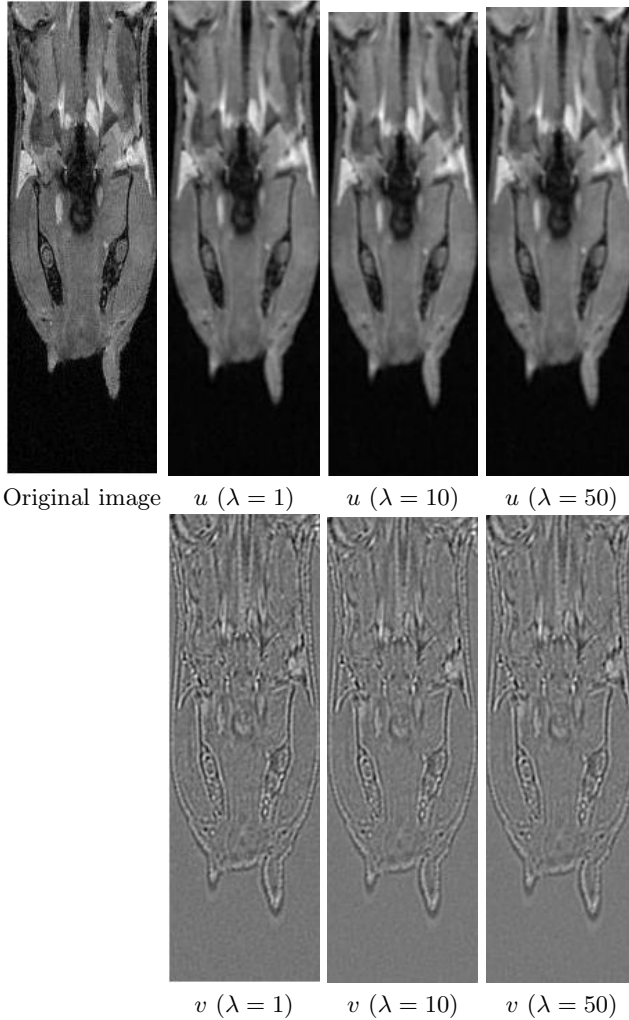
Fig. 1. Original 3D MRI of a Mouse Brain

Original image u $(\lambda = 1)$ u $(\lambda = 10)$ u $(\lambda = 50)$

v $(\lambda = 1)$ v $(\lambda = 10)$ v $(\lambda = 50)$

Fig. 2. Comparison of the $u + v$ decomposition for different value of regulizer λ

One can observe that the algorithm is able to separate the initial MRI image into a component u that contains the regularized (denoised) image, and a component v that contains mostly noise with some texture and contours information. The good ability to denoise the initial 3D image is confirmed on figure 3, which

shows one slice on the 3D image represented as a 2D surface, its regularized component u and its noise component v ($\lambda = 10$). In figure 3, component v can be viewed as a very highly oscillating function. In addition, one can notice in the denoise part that edges are not oversmoothed. Moreover, its behaviour is quite stable with respect to λ (for a large value of $\lambda = 100$, geometric details appear in the noise component v).
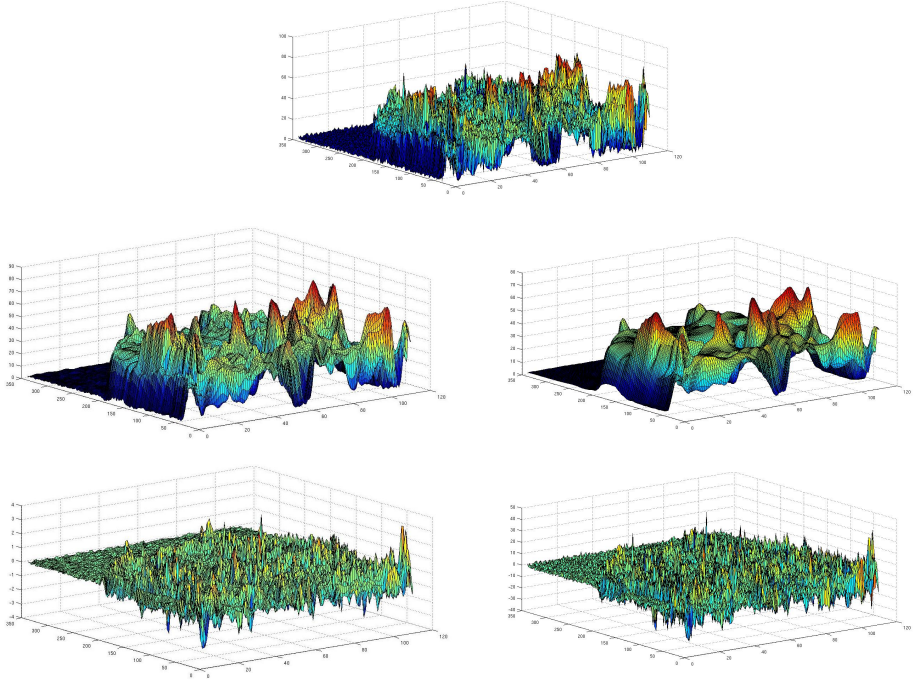

Fig. 3. Surface representation of one slice of the original 3D volume (top). The u component (middle row) and its v component (bottom row). The proposed decomposition model with undecimated wavelet shrinkage (left column) and a comparison with no wavelet shrinkage (right column).

A comparison using the same decomposition model without undecimated wavelet shrinkage has also been performed (using the same value for $\lambda = 10$). It can be noticed on Fig. 3 (right column), that the u component is a bit over-smoothed and thus region borders are blurred.

5   Conclusion

This article describes a new 3D decomposition method which separates a 3D image into two components: the first one containing the geometrical structure of the image, the second one containing the noise. The proposed method is based on a second

order variational model and an undecimated wavelet thresholding operator. The numerical implementation is described, and an experiment for denoising a 3D MRI image of a mouse brain has been successfully performed. In future works, we shall focus on extending this model to a three component model $f = u + v + w$, which could discriminate between geometrical structures (u), textures (v) and noise (w). Application of this method to video is also under consideration.

References

1. Bergounioux, M.: On Poincare-Wirtinger inequalities in spaces of functions of bounded variation. [hal-00515451] version 2 (June 10, 2011)
2. Chambolle, A.: An algorithm for total variation minimization and applications. Journal of Mathematical Imaging and Vision 20, 89–97 (2004)
3. Holschneider, M., Kronland-Martinet, R., Morlet, J., Tchamitchian, P.: A real time algorithm for signal analysis with the help of the wavelet transform. In: Wavelets, Time-Frequency Methods and Phase Space, pp. 286–297. Springer, Berlin (1989)
4. Chambolle, A., Lions, P.L.: Image recovery via total variation minimization and related problems Numerische Mathematik. Journal of Mathematical Imaging and Vision 77, 167–188 (1997)
5. Chan, T., Esedoglu, S., Park, F., Yip, A.: Recent Developments in total Variation Image Restoration. CAM Report 05-01, Department of Mathematics, UCLA (2004)
6. Louchet, C.: Variational and Bayesian models for image denoising: from total variation towards non-local means. Universite Paris Descartes, Ecole Doctoranle Mathematiques Paris-Centre (December 10, 2008)
7. Ekeland, I., Remam, R.: Analyse convex et problemes variationnels. Etudes Mathematiques. Dunod (1974)
8. Aujol, J.-F., Chambolle, A.: Dual norms and image decomposition models. IJCV 63(1), 85–104 (2005)
9. Piffet, L.: Décomposition d'image par modèles variationnels - Débruitage et extraction de texture. Université d'Orléans, Pôle Universités Centre Val de Loire (Novembre 23, 2010)
10. Bergounioux, M., Tran, M.P.: A second order model for 3D texture extraction. In: Mathematical Image Processing. Springer Proceedings in Mathematics, vol. 5. Universite d'Orleans (2011)
11. Starck, J.-L., Candes, E.J., Donoho, D.L.: The Curvelet transform for Image Denoising. IEEE Transactions on Image Processing 11(6) (June 2002)
12. Mallat, S.: A wavelet tour of signal processing. Academic Press Inc. (1998)
13. Jin, Y., Angelini, E., Laine, A.: Wavelets in medical image processing: denoising, sementation and registration. Department of Biomedical Engineering, Columbia University, New York, USA
14. Meyer, Y.: Oscillating patterns in image processing and in some nonlinear evolution equations. The 15th Dean Jacquelines B. Lewis Memorial Lectures (March 2001)
15. Steidl, G., Weickert, J., Brox, T., Mrzek, P., Welk, M.: On the equivalence of soft wavelet shrinkage, total variation diffusion, total variation regularization, and sides, Tech. Rep. 26, Department of Mathematics, University of Bremen, Germany (2003)